CHEMISTRY
A EUROPEAN JOURNAL

DOI: 10.1002/chem.200901668

Synthesis and Crystallochromy of 1,4,7,10-Tetraalkyltetracenes: Tuning of Solid-State Optical Properties of Tetracenes by Alkyl Side-Chain Length

Chitoshi Kitamura,*[a] Yasushi Abe,[a] Takuya Ohara,[a] Akio Yoneda,[a] Takeshi Kawase,[a] Takashi Kobayashi,[b] Hiroyoshi Naito,[b] and Toshiki Komatsu[c]

Abstract: We synthesized a series of 1,4,7,10-tetraalkyltetracenes using a new 2,6-naphthodiyne precursor and 2,5-dialkylfurans as starting materials (alkyl = methyl to hexyl). Surprisingly, the solid-state color of the tetracenes ranges through yellow, orange, and red. Both yellow and red solids are obtained for the butyl derivative. Optical properties in solution show no marked differences; however, those in the solid state show characteristics that vary with alkyl side-chain length: methyl, propyl, and pentyl derivatives are orange; ethyl and butyl derivatives are yellow; and another butyl and hexyl derivative are red. X-ray analyses reveal that the molecular structures are planar, semi-chair, or chair forms; the chair form takes a herringbone-like arrangement and the other forms take slipped parallel arrangements. The mechanism of crystallochromy is discussed in terms of molecular structure, crystal packing, and calculations that take account of exciton coupling.

Keywords: alkyl chains · conformational polymorphism · crystallochromy · exciton coupling · tetracenes

Introduction

Acenes are polycyclic aromatic hydrocarbons that consist of fused benzene rings. Acene molecules, particularly tetracene and pentacene, have recently been receiving increasing attention owing to their excellent electronic performances as organic semiconductors in organic field-effect transistors, organic light-emitting diodes, and organic photovoltaic cells.[1] However, these molecules suffer from some drawbacks, such as low solubility in solution, instability in air, and poor thin-film morphology, which limit their practical application.

To achieve low-cost solution processability with high performance, it is necessary to improve acene solubility in organic solvents and control acene arrangements in the solid state, and hence the tunability of acene physical properties. As a result, a number of organic chemists have performed studies on functionalized tetracenes[2] and pentacenes.[3]

In recent years, we reported the synthesis, crystal structures, and solid-state fluorescence of 1,4,5,8-tetraalkylanthracenes and concluded that the alkyl side-chain length significantly affects alkyl conformation, packing pattern, and fluorescence quantum yield in the crystalline state.[4] We found that the alkyl side chain affects not only solubility, but also the solid-state structural and photophysical properties. In relation to our study on the effects of the alkyl side chain in anthracene, we focused our attention on the effects of the tetracene alkyl side chain on molecular arrangements and optical properties in the solid state. We started to prepare tetracenes **1a–f** with a systematic length variation from methyl to hexyl. To our surprise, we observed crystallochro-

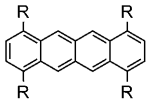

1a: R = CH_3
1b: R = C_2H_5
1c: R = C_3H_7
1d: R = C_4H_9
1e: R = C_5H_{11}
1f: R = C_6H_{13}

[a] Prof. Dr. C. Kitamura, Y. Abe, T. Ohara, Prof. Dr. A. Yoneda, Prof. Dr. T. Kawase
Department of Materials Science and Chemistry
University of Hyogo
2167 Shosha, Himeji, Hyogo 671-2280 (Japan)
Fax: (+81) 79-267-4888
E-mail: kitamura@eng.u-hyogo.ac.jp

[b] Dr. T. Kobayashi, Prof. Dr. H. Naito
Department of Physics and Electronics
Osaka Prefecture University
1–1 Gakuen-cho, Naka-ku, Sakai, Osaka 599-8531 (Japan)

[c] Dr. T. Komatsu
Goi Research Center
Chisso Petrochemical Corporation
5–1 Goikaigan, Ichihara, Chiba 290-8551 (Japan)

Supporting information for this article is available on the WWW under http://dx.doi.org/10.1002/chem.200901668.

my, that is, a dependence of color on different molecular packing, which has been reported for many pigments, particularly perylene-bis(dicarboxyimide) pigments.[5] The color of **1a–f** in the solid state ranges from yellow to red. A recently published preliminary report indicated that **1d** exists as two conformational polymorphic forms composed of yellow and red solids.[6]

In this paper, we describe the synthesis of a series of alkyl-substituted tetracenes **1a–f**, optical properties of the tetracenes in the solid state, and X-ray crystallographic analyses. We also discuss a possible mechanism for solid-state color change governed by the alkyl side-chain length.

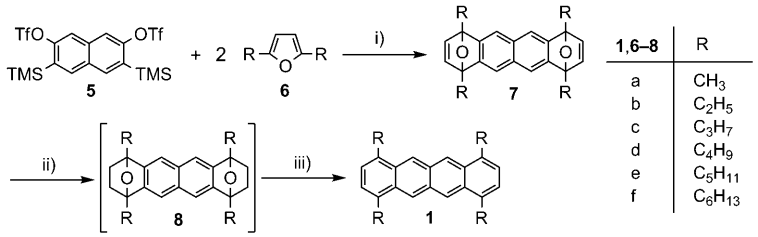

Scheme 2. Synthesis of tetracenes **1a–f**: i) KF, [18]crown-6, THF, RT, 27–72%; ii) H_2, 10% Pd/C, *n*BuOH, RT; iii) HCl, Ac_2O, RT, 27–55% from **7a–f**.

Results and Discussion

Synthesis of 1,4,7,10-tetraalkyltetracenes: Gribble et al. have reported the preparation of tetramethyltetracene **1a** by Diels–Alder cycloaddition of 2,5-dimethylfuran and 2,6-naphthodiyne synthon, the latter produced from 3,6-dibromo-2,7-bis(*p*-tosyloxy)naphthalene in situ.[7] This methodology was unsatisfactory for our purposes because the yields of Diels–Alder cycloadduct having longer alkyl chains decline significantly (≈10%) with increasing alkyl side-chain length. Considering that this decline was due to the relatively low reaction temperature (0°C) and the use of an active reagent *n*BuLi, we were able to improve the method. Fluorine-induced benzyne formation from *o*-trimethylsilylphenyl triflate can occur under mild conditions, for example, at room temperature,[8] and is currently widely used in organic reactions.[9,10] A bis(benzyne) precursor has also been prepared by Wudl et al.[11] We adapted their methods to prepare a new bis(aryne) precursor **5** (Scheme 1). Treatment of 3,6-dibromo-2,7-dihydroxynaphthalene[12] (**2**) with trimethylsilyl chloride (TMSCl) in pyridine and toluene at reflux resulted in a 90% yield of the corresponding trimethylsilyl ether **3**. Reaction of **3** with *n*BuLi and subsequently with TMSCl in THF at −80°C yielded **4** in 74% yield. Further treatment of **4** with *n*BuLi in Et_2O at 0°C and quenching with trifluoromethanesulfonic anhydride (Tf_2O) gave bis-(triflate) **5** in 78% yield. Compound **5** was stored in a freezer and used as soon as possible because of slight instability. Tetracenes **1a–f** were prepared as shown in Scheme 2. Slow generation of the 2,6-naphthodiyne synthon by room-temperature treatment of **5** with excess 2,5-dialkylfurans (**6a–f**) in the presence of KF and [18]crown-6 in THF afforded Diels–Alder cycloadducts **7a–f** in 27–72% yields. Although adducts **7a–f** can exist as a mixture of *syn* and *anti* isomers, they behaved as a single compound, and the *syn* and *anti* isomers were indistinguishable from each other. Hydrogenation of **7a–f** with 10% Pd/C in *n*BuOH and subsequent treatment with acetic anhydride and conc. HCl gave tetracenes **1a–f** in 27–55% yields with respect to **7a–f**. The tetracenes were soluble in common organic solvents; an alkyl side chain longer than a propyl group greatly increased the solubility.

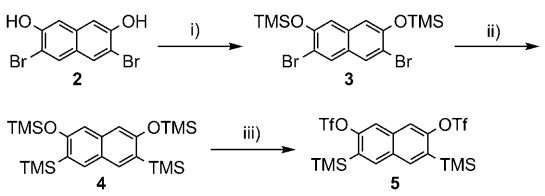

Scheme 1. Synthesis of bis(aryne) precursor **5**. i) TMSCl, pyridine, toluene, reflux, 90%; ii) a) *n*BuLi, THF, −80°C, b) TMSCl, −80°C to RT, 74%; iii) a) *n*BuLi, Et_2O, 0°C, b) Tf_2O, 0°C, 78%.

During synthesis of tetracenes **1a–f**, we encountered the following unexpected findings: 1) The solid-state color of the tetracenes was yellow (**1b**), orange (**1a, 1c**, and **1e**), and red (**1f**). 2) The solid-state color of butyl derivative **1d** was a mixture of red and yellow, and the two colors (form A or form B) could be separated by evaporation from chloroform or hexane solution, respectively.[6] The images in Figure 1 show this solid-state crystallochromic effect for the alkyl-substituted tetracene series—to our knowledge, the first case of crystallochromy among acenes. The colors range from yellow (ethyl (**1b**) and butyl (**1d**-form B) derivatives) to orange (methyl (**1a**), propyl (**1c**), and pentyl (**1e**) deriva-

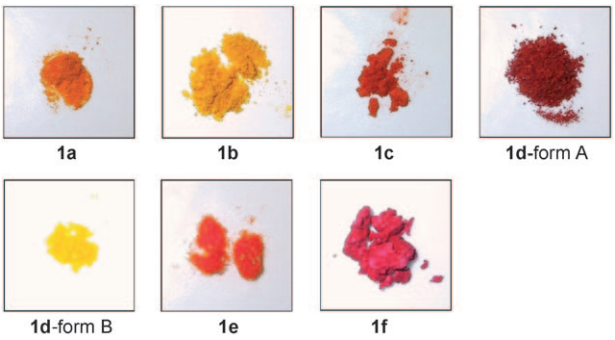

Figure 1. Photographs of tetracenes **1a–f** in powder form.

tives) to red (butyl (**1d**-form A) and hexyl (**1f**) derivatives). Thus, color in the solid state seems to be closely correlated with alkyl side-chain length.

Optical properties of 1,4,7,10-tetraalkyltetracenes in solution and in the solid state: UV/Vis absorption and fluorescence spectra for **1a–f**, both in hexane and in the solid state, are shown in Figure 2. Spectral data are summarized in Table 1 and Table 2.

In solution, **1a–f** do not exhibit marked differences with respect to spectral shape, wavelengths of absorption and fluorescence peaks, and fluorescence quantum yield (Φ_F values are around 0.1). We assume that the molecules exist in a practically monodispersed state in a dilute solution. Both absorption and fluorescence spectra show vibrational structures such as 0–0, 0–1, and 0–2 transitions. The longest wavelengths of maximum absorption are around 474–482 nm, and the shortest wavelengths of maximum fluorescence are around 483–495 nm. In both spectra, the maximal peaks exhibit a slight red shift with increasing alkyl chain length; values are constant when the alkyl side chain is longer than a propyl group.

Table 1. UV/Vis absorption and fluorescence properties of **1a–f** in hexane.

Compound	Absorption λ_{max}[a] [nm] (log ε)	Fluorescence λ_{em}[b] [nm]	Φ_F[c]
1a	419 (3.56), 445 (3.81), 474 (3.81)	483, 512, 548	0.09
1b	422 (3.65), 446 (3.87), 478 (3.88)	490, 520, 554	0.10
1c	424 (3.64), 451 (3.88), 481 (3.88)	493, 523, 558	0.08
1d	425 (3.63), 452 (3.80), 482 (3.79)	495, 524, 558	0.09
1e	425 (3.62), 452 (3.77), 482 (3.77)	495, 524, 560	0.10
1f	425 (3.67), 452 (3.92), 482 (3.92)	495, 524, 560	0.10

[a] Peaks based on the 0–0, 0–1, and 0–2 transitions. [b] Excited at 365 nm. [c] Fluorescence quantum yields were determined using 9,10-diphenylanthracene as the standard.

In the solid state, the spectral shape of absorption (Kubelka–Munk) and fluorescence as well as the quantum yield differ among **1a–f**. Except for **1c** and **1f**, the absorption spectra in a diluted KBr pellet show structured bands. The longest wavelengths of maximum absorption are as follows: 491 nm for **1a**, 485 nm for **1b**, 569 nm for **1d**-form A, 484 nm for **1d**-form B, and 513 nm for **1e**. In addition, optical absorption edges are in the following order: **1b** (537 nm) < **1d**-form B (552 nm) < **1a** (560 nm) < **1c**

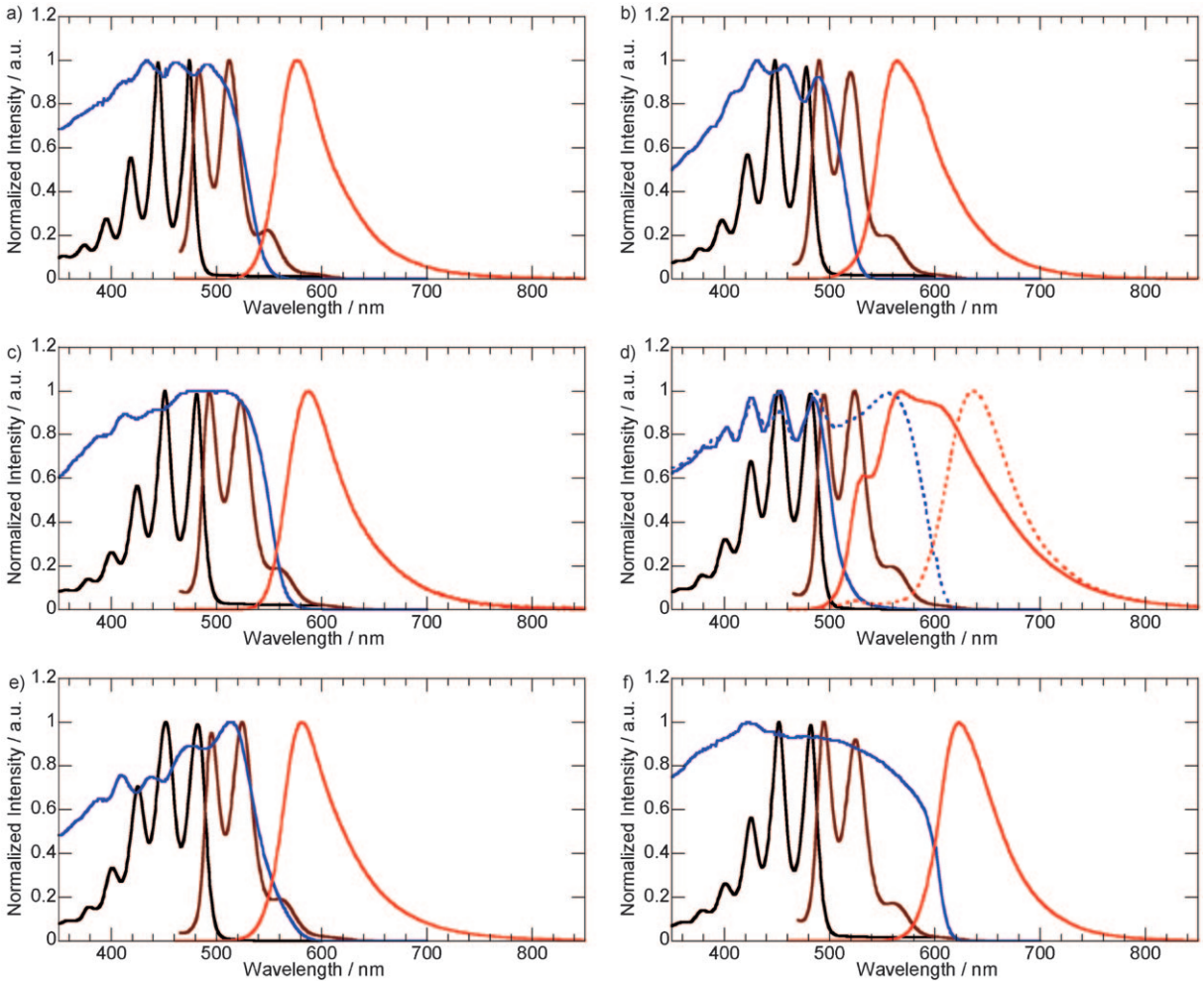

Figure 2. UV/Vis absorption (solution: black, and solid: blue) and fluorescence (solution: brown, and solid: red) spectra of tetracenes, a) **1a**, b) **1b**, c) **1c**, d) **1d** (form A: ·····, and form B: ——), e) **1e**, and f) **1f**.

Table 2. UV/Vis absorption and fluorescence properties of **1a**–**f** in the solid state.

Compound	Absorption[a]		Fluorescence	
	λ_{max} [nm]	λ_{edge} [nm]	λ_{em}[b] [nm]	Φ_F[c]
1a	491	560	578	0.21
1b	485	537	564	0.40
1c	–[d]	580	588	0.22
1d-form A	569	619	637	0.16
1d-form B	484	552	529, 569, 599	0.34
1e	513	588	581	0.13
1f	–[d]	620	623	0.20

[a] Kubelka–Munk spectra of a diluted pellet. [b] Excited at 325 nm. [c] Absolute quantum yield in the solid state. [d] Maximum peak was not observed.

(580 nm) < **1e** (588 nm) < **1d**-form A (619 nm) < **1f** (620 nm). This order correlates well with the solid-state colors. In analyzing these data, we can definitely recognize structural regularity of the alkyl side-chain length, resembling the odd-even effect frequently seen in liquid crystals.[13] The numbers of carbon atoms in the alkyl side chain are as follows: 2 and 4 for yellow solids; 1, 3, and 5 for orange solids; and 4 and 6 for red solids.

Furthermore, considerable differences in the fluorescence of the powder form are also evident. All the tetracenes except **1d**-form B exhibit three bands, grouped into one broad band whose peak is in the range 564–637 nm. The wavelengths of maximum fluorescence are in the following order: **1b** (564 nm) < **1d**-form B (569 nm) < **1a** (578 nm) < **1e** (581 nm) < **1c** (588 nm) < **1e** (623 nm) < **1d**-form A (637 nm). Similar to the case of solid-state absorption, the substances with more red-shifted color exhibit a longer fluorescence maximum. The fluorescence quantum yields (Φ_F = 0.13–0.40) are larger than those of solutions.

It is reasonable that differences in the solid-state optical properties among molecules having fixed alkyl side chains in the solid state should derive from differences in their aggregation patterns.

Crystal structures: To clarify the essence of crystallochromy, that is, the correlation of crystal packing with solid-state color and alkyl side-chain length, we performed X-ray crystallographic analyses. Molecular structures, stacking patterns of two neighboring molecules, and packing diagrams are shown in Figures 3–5. All of the molecules possess a center of symmetry, and halves of the formula units are crystallographically independent because of the high symmetry of the molecules (Figure 3). The tetracene frameworks are strictly planar. We can thus obtain a spectacular view of their molecular structures, namely conformational polymorphism accompanied by different alkyl side-chain conformations.[14]

In the first step, we categorized the alkyl side-chain conformations into three groups: a planar form for **1b** and **1d**-form B (Figure 3b,e), a semi-chair form for **1c** and **1e** (Figure 3c,f), and a chair form for **1d**-form A and **1f** (Figure 3d,g). As we already reported, **1d**-form A and **1d**-form B are conformational polymorphs of the same molecule.[6] Interestingly, solids with similar molecular structures have similar colors: **1b** and **1d**-form B are yellow; **1c** and **1e** are orange; and **1d**-form A and **1f** are red. All of the alkyl side chains take an all-trans planar conformation. In the planar form, the alkyl chains at the 1-, 4-, 7-, and 10-positions take a coplanar conformation with the tetracene ring. In the chair form, a pair of alkyl groups at the 1- and 10-positions extends upward and another pair of alkyl groups at the 4- and 7-positions extends downward out of the tetracene plane. The semi-chair form looks like an intermediate conformer between the planar and chair forms. A pair of alkyl groups at the 1- and 7-positions takes a coplanar conformation with the tetracene ring and another pair of alkyl groups at the 4- and 10-positions extends upward and downward out of the tetracene plane. The three conformations must contribute to the torsion degrees of freedom in the alkyl chain. As shown below for molecular orbital (MO) calculations, the molecular structure alone cannot explain the

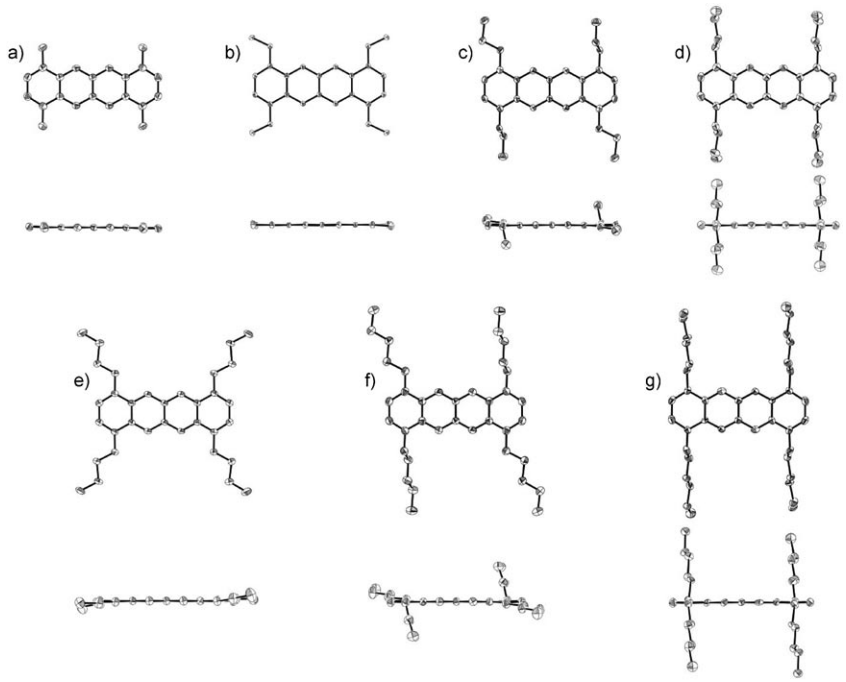

Figure 3. Molecular structures of a) **1a**, b) **1b**, c) **1c**, d) **1d**-form A, e) **1d**-form B, f) **1e**, and g) **1f**.

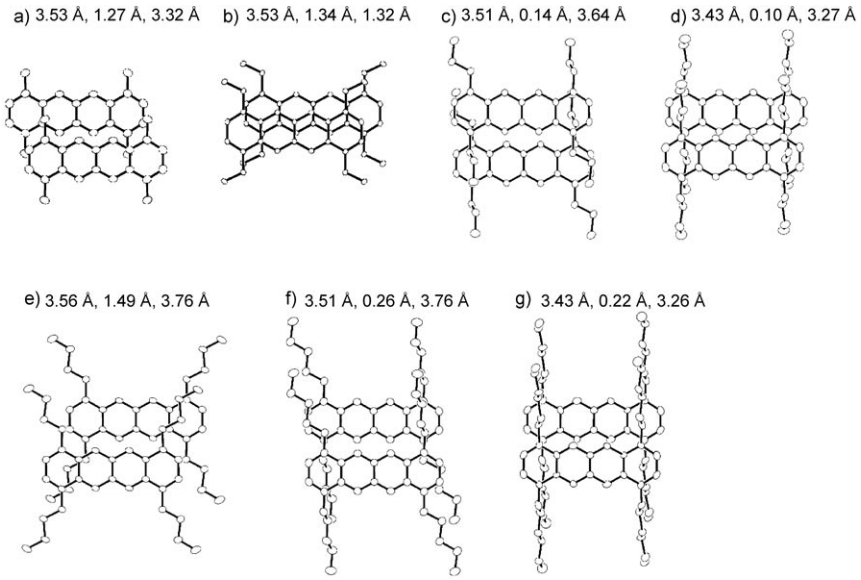

Figure 4. Stacking patterns of two vicinal molecules of a) **1a**, b) **1b**, c) **1c**, d) **1d**-form A, e) **1d**-form B, f) **1e**, and g) **1f**. The three numbers above each diagram indicate the stacking distance (*d*) between neighboring molecules, the longitudinal (*l*) and transverse (*t*) shifts.

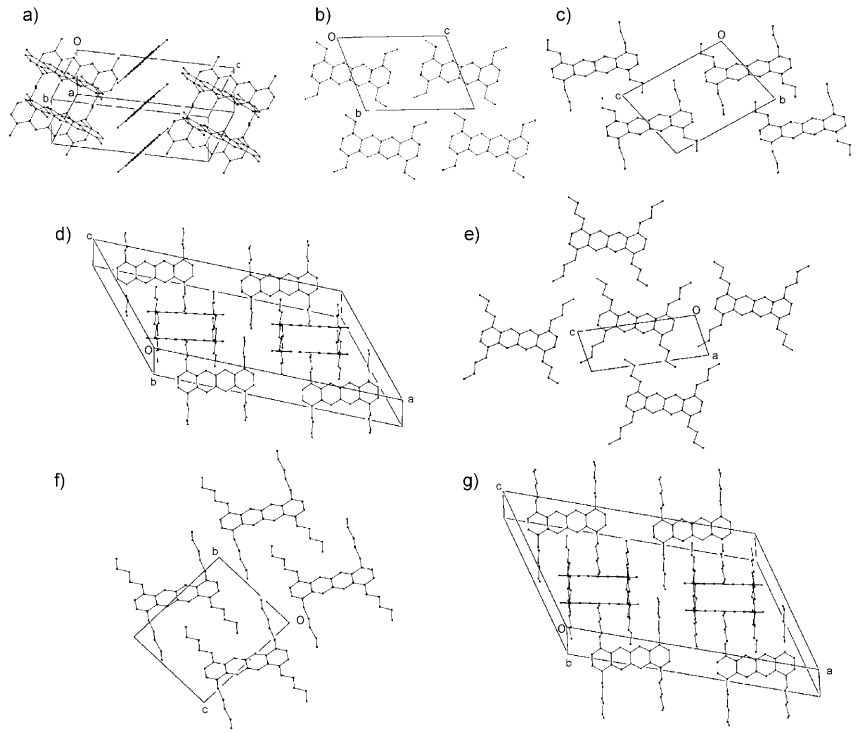

Figure 5. Packing diagrams of a) **1a**, b) **1b**, c) **1c**, d) **1d**-form A, e) **1d**-form B, f) **1e**, and g) **1f**.

difference in color in the solid state. Therefore, mechanisms derived from intermolecular interactions must be considered for understanding the solid-state color.

Next, we examined stacking patterns of two neighboring molecules along the one-dimensional (1D) stacking direction in the crystal (Figure 4), as previously carried out by Graser[5a] and Kazmair[15] in analyzing the crystallochromy of perylene pigments. We surveyed the geometrical parameters of tetracene interplanar spacing (*d*), longitudinal shift (*l*), and transverse shift (*t*). The *d* distance is 3.43–3.56 Å, and there is not much difference among the tetracene molecules. In contrast, there are a variety of *l* and *t* shifts. The *l* shifts for **1a**, **1b**, and **1d**-form B (1.27, 1,34, and 1.49 Å, respectively) are longer than those for **1c**, **1d**-form A, **1e**, and **1f** (0.14, 0.10, 0.26, and 0.22 Å, respectively). The *t* shift for **1b** (1.32 Å) is the shortest, reflecting the presence of π–π overlap. Other *t* shifts range from 3.26 to 3.76 Å. Although only **1b** looks special, it is not special with respect to solid-state optical properties. That is, **1b** and **1d**-form B are similar in color. This suggests that there is a small relationship between one small part of the three-dimensional (3D) crystal packing and the color in the solid state using a function of the above three parameters.

The 3D crystal packing intuitively affords much more valuable information (Figure 5). Molecules of **1a**, **1d**-form A, and **1f** are stacked in a herringbone-like fashion. In both **1d**-form A and **1f**, two alkyl chains at the same *peri* position are interdigitated with two other alkyl chains of the neighboring molecule in another stacking column. In contrast, molecules of **1b**, **1c**, **1d**-form B, and **1e** adopt a slipped-parallel arrangement of stacked molecular sheets. Viewed perpendicularly to the molecular sheet, π–π overlap is not observed except for **1b**. The nature of the crystal packing probably depends on the balance of intermolecular interactions between tetracene moieties, such as face-to-face (π–π stacking) and edge-to-face (CH–π) interactions, and on the degree of self-assembly of the alkyl side chain. Similarity in molecular arrangement is obvious between **1b** and **1d**-form B, between **1c** and **1e**, and between **1d**-form A and

1f. Although **1a** is an exceptional instance, it is definitely valid that similar crystal packing correlates with similar color in the solid state. Because, in the solid state, there is no relationship between overlapping mode and color, but significant correlation between crystal packing and color, we conclude that intermolecular interactions affect color. We think that color in the solid state closely relates to alkyl side-chain length, alkyl conformation, and molecular arrangement of the side chain. In other words, the length of the alkyl side chain can control alkyl conformation to give conformational polymorphs. Moreover, the individual polymorphs behave as Lego blocks to assemble unique molecular aggregates, which ultimately define the solid-state color.

MO calculations of the lowest-energy absorption band: It is well known that it is almost impossible to estimate color from the crystal packing pattern. There is no effective method to precisely evaluate optical properties in the solid state. We thus performed MO calculations to determine the lowest-energy absorption band of the crystals and to better understand the tuning of color in the solid state by alkyl side-chain length. Alkyl chains themselves do not absorb visible light at all. Therefore, they can act as spacers and modulate the spatial arrangements of tetracene moieties.

First, on the basis of the geometries determined by X-ray analysis, we calculated the lowest-energy absorption band for each alkyl-substituted tetracene (E_1) at a single molecular level using time-dependent density functional theory (TD-DFT) and the B3LYP/6-31G* method (Table 3). Deviations for E_1 are in the range 472.1–499.1 nm, which may contain electronic effects derived from alkyl conformations. E_1 values exhibit a few contradictions with respect to the actual color tones of the solids. Although **1b** is yellow, its E_1 value (490.1 nm) is more red-shifted than are the values for the others. Similarly, although **1c** is orange, its E_1 value (480.9 nm) is more blue-shifted than are the values for the orange **1a** (486.5 nm) and **1e** (490.6 nm). These calculations do not strictly agree with the actual colors of the solids, indicating the computational limit at the single molecular level.

We thus assumed that a correction based on intermolecular interactions is required to raise the precision of the MO calculations. Kasha applied molecular exciton theory to explain the electronic properties of 1D molecular aggregates such as *J* and *H* aggregates.[17] The essential point of molecular exciton theory is that, from intermolecular interactions between transition dipole moments in a pair of molecules (dimer model), spectroscopic change (blue or red shift) and band splitting (Davydov splitting) arise, which are dependent upon mutual orientation and separation of the two molecules. Kasha introduced a simple model of point-dipole approximations for exciton coupling that is user-friendly and provides fast qualitative predictions,[18] similar to the simple Hückel MO approximation. A couple of groups[19,20] have already applied point-dipole approximations to predict the color of dyes and pigments in a crystal.

In a crystal, exciton coupling is assumed to involve energy contributions from interactions with all nearest-neighbor molecules. Taking into account these interactions and the geometries of the crystals, we calculated total exciton displacement energies ($\Delta E_{exciton}$) for **1a–f**. Results of these calculations, listed in Table 3, show clearly that yellow **1b** and **1d**-form B have positive (blue) shifts (0.0493 and 0.0032 eV, respectively) and the others have negative (red) shifts (−0.0092 to −0.0211 eV). This suggests that characteristic crystal packing is the main cause of the spectral shifts. The absorption band (E_2), corrected by taking into account exciton coupling, is in the range 471.2–501.3 nm, suggesting a better improvement over E_1. E_2 values for yellow **1b** and **1d**-form B are 480.4 and 471.2 nm, respectively; values for orange **1a**, **1c**, and **1e** are 488.0, 484.3, and 494.4 nm, respectively; and values for red **1d**-form A and **1f** are 501.3 and 500.6 nm, respectively.

Although there is a gap between E_2 and actual absorption spectra in the solid state, we believe that, in the alkyl-substituted tetracene system, calculations involving exciton coupling provide a rough guideline for understanding the relationship between optical properties in the solid state and molecular arrangement in the crystal, and serve as a valuable tool for predictions of spectral shifts.

Table 3. Calculated absorption bands.

Compound	Color in the solid state	E_1[a]		E_{shift}[b]	E_2[c]	
		Energy [eV]	Wavelength [nm]	Shift [eV]	Energy [eV]	Wavelength [nm]
1a	orange	2.5484	486.5	−0.0092	2.5392	488.0
1b	yellow	2.5296	490.1	0.0493	2.5789	480.4
1c	orange	2.5781	480.9	−0.0198	2.5583	484.3
1d-form A	red	2.4842	499.1	−0.0127	2.4715	501.3
1d-form B	yellow	2.6262	472.1	0.0032	2.6294	471.2
1e	orange	2.5272	490.6	−0.0211	2.5061	494.4
1f	red	2.4857	498.8	−0.0109	2.4747	500.6

[a] The lowest-energy absorption band at the single molecular level calculated by TD-DFT (B3LYP/6-31G*) using the geometry obtained by X-ray analysis. [b] Total exciton displacement energy. [c] $E_2 = E_1 + E_{shift}$.

Conclusions

1,4,7,10-Tetraalkyltetracenes (**1a–f**) were synthesized by a Diels–Alder reaction between a new bis(aryne) precursor **5** and 2,5-dialkylfurans (**6a–f**) in the presence of KF and [18]crown-6 in THF. The color of the tetracenes in the solid state ranges from yellow to red. The alkyl side-chain length plays a crucial role in determining optical properties in the solid state, although there is no significant difference in optical properties in solution. In the case of butyl derivative **1d**, a mixture of yellow and red solids was obtained, and each component was isolated. Structural information for all molecules was characterized by X-ray analysis. Differing alkyl side-chain lengths cause differ-

ing alkyl conformation, and thus differing molecular structures—planar, semi-chair, or chair form—although all the alkyl chains take an all-*trans* planar conformation. Crystal packing is herringbone-like in the red solid and has a slipped-parallel arrangement in the orange and yellow solids. The packing arrangements for solids of the same color are similar to one another. MO calculations based on the geometry obtained by X-ray analysis gave unsatisfactory results for the lowest-energy absorption band. However, calculated spectral shifts based on exciton coupling afforded qualitatively good agreement with experimental results. We expect that the technique for varying the alkyl side-chain length can be used for other chromophores, dyes, and pigments to allow tuning of the optical properties in the solid state.

Experimental Section

General: 3,6-Dibromo-2,7-dihydroxynaphthalene[12] (**2**) was synthesized by previously described procedures. 2,5-Dimethylfuran and all other reagents were commercially available and used without further purification. Solvents for syntheses were purified by standard methods. Column chromatography was performed by using Wako silica gel C-300 (45–75 μm). Melting points were measured on a Yanaco melting point apparatus. ^{1}H and ^{13}C spectra were measured by using a Bruker-Biospin DRX500 FT spectrometer. Absorption and fluorescence spectra in solution were recorded with a HITACHI U3500 spectrophotometer and a HITACHI F2500 spectrophotometer, respectively. Fluorescence yields (Φ_F) in solution were determined with 9,10-diphenylanthracene ($\Phi_F = 0.86$)[21] in cyclohexane as the standard. Elemental analyses were carried out on a Yanaco MT-5 CHN analyzer. Kubelka–Munk spectra were measured using a HITACHI U3010 spectrophotometer with a Φ60 integrating sphere attachment. Fluorescence spectra in the solid state were recorded using a Hamamatsu Photonics PMA11 calibrated optical multichannel analyzer ($\lambda_{ex} = 325$ nm), and the absolute quantum yield (Φ_F) was measured with a Labsphere IS-040-SF integrating sphere.

Preparation of bis(aryne) precursor 5: A mixture of 3,6-dibromo-2,7-dihydoroxynaphthalene[12] (**2**; 6.28 g, 19.8 mmol) and toluene (60 mL) was heated until **2** dissolved completely. After addition of a solution of TMSCl (18 mL) and pyridine (18 mL), the mixture was stirred at reflux for 18 h, then cooled to room temperature. Water was cautiously added, and the organic layer was separated, washed with brine, and dried over Na_2SO_4. Hexane was added to the organic solution, and the mixture was filtered to remove resultant deposition. After removal of solvents and vacuum drying, **3** was obtained as a creamy white solid (8.23 g, 90% yield) and used in the next reaction without further purification. M.p. 81–83 °C; ^{1}H NMR (500 MHz, $CDCl_3$): $\delta = 0.36$ (s, 18H), 7.05 (s, 2H), 7.89 ppm (s, 2H); ^{13}C NMR (126 MHz, $CDCl_3$): $\delta = 0.34$, 114.29, 115.67, 126.58, 130.79, 133.76, 150.48 ppm. To a solution of **3** (2.83 g, 6.11 mmol) in THF (15 mL), 1.6 M *n*BuLi in hexane (9 mL, 14.4 mmol) was added dropwise at −80 °C. The mixture was stirred for 30 min at −80 °C. TMSCl (2.5 mL, 19.6 mmol) was added dropwise. The mixture was allowed to warm to room temperature and was then stirred for an additional 17 h. Water was cautiously added, and the resulting mixture was extracted with Et_2O. The combined organic layers were washed with brine and dried over Na_2SO_4. After removal of solvents, MeOH was added to the residue, and the resulting solid was filtered off. After vacuum drying, **4** was obtained as a white solid (2.01 g, 74% yield) and used in the next reaction without further purification. M.p. 142–144 °C; ^{1}H NMR (500 MHz, $CDCl_3$): $\delta = 0.30$ (s, 18H), 0.39 (s, 18H), 6.84 (s, 2H), 7.76 ppm (s, 2H); ^{13}C NMR (126 MHz, $CDCl_3$): $\delta = -0.74$, 0.68, 109.58, 124.38, 129.77, 136.25, 137.60, 158.58 ppm. To a solution of **4** (1.03 g, 2.03 mmol) in Et_2O (15 mL), 1.6 M *n*BuLi in hexane (5 mL, 8.0 mmol) was added dropwise at 0 °C. The mixture was allowed to warm to room temperature and was then stirred for an additional 4 h. After cooling to 0 °C again, Tf_2O (1.5 mL, 8.92 mmol) was added over 5 min, and the mixture was stirred at 0 °C for an additional 30 min. A saturated solution of $NaHCO_3$ in water was cautiously added, and the resulting mixture was extracted with Et_2O. The combined organic layers were washed with brine and dried over Na_2SO_4. After removal of solvents and drying under vacuum, **5** was obtained as a brown solid (1.03 g, 78% yield) and used in the next reaction without further purification. *Caution!* **5** is slightly unstable at room temperature. Therefore, **5** should be stored in a freezer. It is advisable to use **5** within one week in the next Diels–Alder reaction. M.p. 70–72 °C; ^{1}H NMR (500 MHz, $CDCl_3$): $\delta = 0.44$ (s, 18H), 7.80 (s, 2H), 8.04 ppm (s, 2H); ^{13}C NMR (126 MHz, $CDCl_3$): $\delta = -0.86$, 116.27, 118.69 (q, $J =$ 320 Hz), 130.02, 132.76, 135.03, 137.63, 153.70 ppm; elemental analysis calcd (%) for $C_{18}H_{22}F_6O_6S_2Si_2$: C 38.02; H 3.90; found: C 38.32, H 3.84.

General procedure for the preparation of 2,5-dialkylfurans 6b–f: These compounds ($R = C_2H_5$ to C_6H_{13}) were synthesized using our recently reported procedure.[21] To an ice-cooled mixture of furan (2.0 mL, 1 equiv, 27.6 mmol) and TMEDA (9.4 mL, 2.2 equiv, 62.3 mmol), 1.6 M *n*BuLi in hexane (40 mL, 2.2 equiv, 61.6 mmol) was added slowly, and the mixture was refluxed for 1 h. The mixture changed to a brown suspension on heating. The mixture was allowed to cool to RT, and was then cooled with an ice bath. To the ice-cooled mixture, a solution of 1-bromoalkane (3 equiv) in THF (20 mL) was added dropwise. The mixture was stirred at RT overnight. After quenching with water, the crude product was extracted with Et_2O, washed with brine, and dried over Na_2SO_4. After evaporation of the solvents, the residue was subjected to column chromatography ($CHCl_3$/hexane 1:1) on silica gel and dried under a vacuum with mild heating (40–50 °C) to remove unreacted 1-bromoalkane and monosubstituted furan. The di-substituted furans **6b–f** were obtained in 38–44% yields, and used in the next reaction without further purification.

General procedure for the preparation of 1,4,7,10-tetraalkyltetracenes 1a–f: KF (221 mg, 4.4 equiv, 3.80 mmol) was added to a solution of bis(aryne) precursor **5** (496 mg, 1 equiv, 0.87 mmol), dialkylfuran **6a–f** (2 equiv), and [18]crown-6 (956 mg, 4.2 equiv, 3.62 mmol) in THF (10 mL). The mixture was stirred at room temperature for 20 h. Water was added, and the resulting mixture was extracted with Et_2O. The combined organic layers were washed with brine and dried over Na_2SO_4. After removal of the solvents, the residue was purified by column chromatography ($CHCl_3$/hexane 1:1) to afford a mixture of *syn* and *anti* isomers of **7a–f** (yields from **5**: **7a**, 72%; **7b**, 89%; **7c**, 52%; **7d**, 59%, **7e**, 27%, **7f**, 34%) as a pale brown oil. Because **7a–f** are apt to decompose on standing at RT, **7a–f** was used as soon as possible in the next reaction. A solution of **7a–f** in *n*BuOH (20 mL) was hydrogenated over 10% Pd/C (30 mg) under atmospheric pressure at room temperature for 3 h. The catalyst was removed by filtration, and the filtrate was concentrated under reduced pressure. To the residue was added a cold solution of conc HCl (6 mL) and Ac_2O (30 mL) at 0 °C, and the mixture was stirred at room temperature for 1 h. Water was added, and the resulting mixture was extracted with $CHCl_3$. The combined organic layers were washed with brine and dried over Na_2SO_4. After removal of the solvents, column chromatography (hexane) of the residue on silica gel and recrystallization with Et_2O afforded tetracene **1a–f** (yields from **7a–f**: **1a**, 27%; **1b**, 33%; **1c**, 48%; **1d**, 55%, **1e**, 52%, **1f**, 45%). *Caution!* Solutions of **1a–f** are slightly unstable in the presence of both light and air. Therefore they should be handled in the dark. In contrast, **1a–f** in the solid state was stable in the presence of both light and air.

1,4,7,10-Tetramethyltetracene (**1a**): Orange solid (m.p. 276–278 °C; lit.:[7] 269–273 °C); ^{1}H NMR (500 MHz, $CDCl_3$): $\delta = 2.83$ (s, 12H), 7.15 (s, 4H), 8.82 ppm (s, 4H).

1,4,7,10-Tetraethyltetracene (**1b**): Yellow solid (m.p. 189–191 °C); ^{1}H NMR (500 MHz, $CDCl_3$): $\delta = 1.51$ (t, $J = 7.5$ Hz, 12H), 3.28 (q, $J =$ 7.5 Hz, 8H), 7.15 (s, 4H), 8.82 ppm (s, 4H); ^{13}C NMR (126 MHz, $CDCl_3$): $\delta = 14.57$, 25.99, 123.00, 123.13, 129.11, 130.81, 138.05 ppm; elemental analysis calcd (%) for $C_{26}H_{28}$: C 91.71, H 8.29; found C 91.76, H 8.41.

1,4,7,10-Tetrapropyltetracene (**1c**): Orange solid (m.p. 194–196 °C); ^{1}H NMR (500 MHz, $CDCl_3$): $\delta = 1.14$ (t, $J = 7.3$ Hz, 12H), 1.90–1.98 (m, 8H), 3.20 (t, $J = 7.6$ Hz, 8H), 7.18 (s, 4H), 8.85 ppm (s, 4H); ^{13}C NMR (126 MHz, $CDCl_3$): $\delta = 14.50$, 23.34, 35.44, 123.28, 124.05, 129.05, 131.06,

136.58 ppm; elemental analysis calcd (%) for $C_{30}H_{36}$: C 90.85, H 9.15; found C 90.93, H 9.32.

1,4,7,10-Tetrabutyltetracene (**1d**): Mixture of yellow and red solids (m.p. 128–131 °C); ^{1}H NMR (500 MHz, $CDCl_3$): $\delta = 1.03$ (t, $J = 7.3$ Hz, 12H), 1.53–1.57 (m, 8H), 1.84–1.90 (m, 8H), 3.19 (t, $J = 7.8$ Hz, 8H), 7.14 (s, 4H), 8.81 ppm (s, 4H); ^{13}C NMR (126 MHz, $CDCl_3$): $\delta = 14.16$, 23.03, 32.31, 32.95, 123.22, 123.87, 128.99, 131.00, 136.67 ppm; elemental analysis calcd (%) for $C_{34}H_{44}$: C 90.20, H 9.80; found C 90.27, H 9.71. The red solid (form A: m.p. 128–130 °C) was produced by high-rate evaporation using a rotary evaporator from a $CHCl_3$ solution, and the yellow solid (form B: m.p. 114–116 °C) was obtained by rate-independent evaporation using a rotary evaporator from a hexane solution and then manual removal of a small amount of red solid.

1,4,7,10-Tetrapentyltetracene (**1e**): Orange solid (m.p. 129–130 °C); ^{1}H NMR (500 MHz, $CDCl_3$): $\delta = 0.95$ (t, $J = 7.2$ Hz, 12H), 1.41–1.55 (m, 16H), 1.86–1.92 (m, 8H), 3.20 (t, $J = 7.7$ Hz, 8H), 7.14 (s, 4H), 8.81 ppm (s, 4H); ^{13}C NMR (126 MHz, $CDCl_3$): $\delta = 14.15$, 22.68, 29.85, 32.17, 33.20, 123.22, 123.87, 129.00, 130.99, 136.72 ppm; elemental analysis calcd (%) for $C_{38}H_{52}$: C 89.72, H 10.30; found C 89.95, H 10.39.

1,4,7,10-Tetrahexyltetracene (**1f**): Red solid (m.p. 108–109 °C); ^{1}H NMR (500 MHz, $CDCl_3$): $\delta = 0.93$ (t, $J = 7.0$ Hz, 12H), 1.36–1.44 (m, 16H), 1.51–1.56 (m, 8H), 1.86–1.92 (m, 8H), 3.22 (t, $J = 7.7$ Hz, 8H), 7.17 (s, 4H), 8.84 ppm (s, 4H); ^{13}C NMR (126 MHz, $CDCl_3$): $\delta = 14.17$, 22.72, 29.65, 30.14, 31.84, 33.27, 123.26, 123.91, 129.02, 131.01, 136.78 ppm; elemental analysis calcd (%) for $C_{42}H_{60}$: C 89.29, H 10.71; found C 89.44, H 10.60.

X-ray crystallography: Single crystals suitable for X-ray analysis were obtained by slow evaporation from the following solvents: Et_2O-toluene for **1a**, toluene for **1b** and **1d–f**, benzene for **1c**. X-ray diffraction data were collected on a Rigaku/Mercury CCD area-detector diffractometer with graphite-monochromated $Mo_{K\alpha}$ ($\alpha = 0.71070$ Å) radiation, ϕ and ω scans to a maximum 2θ value of 55.0°. The structures were solved by a direct method using SIR92.[22] All non-hydrogen atoms were refined anisotropically by full-matrix least-squares on F^2 using SHELXL97.[23] Hydrogen atoms of **1a-e** were refined isotropically, and those of **1f** were positioned geometrically and refined using a riding model. All calculations were performed using the teXsan program package.[24] CCDC-723050 (**1a**), CCDC-723051 (**1b**), CCDC-723052 (**1c**), CCDC-642337 (**1d**-form A), CCDC-642338 (**1d**-form B), CCDC-723053 (**1e**), and CCDC-723054 (**1f**) contain supplementary crystallographic data for this paper. These data can be obtained free of charge from The Cambridge Crystallographic Data Centre via www.ccdc.cam.ac.uk/data_request/cif.

Crystal data for **1a**: Crystal dimensions: $0.50 \times 0.10 \times 0.05$ mm, $C_{22}H_{20}$, $M = 284.40$, $T = 223$ K, triclinic, space group $P\bar{1}$, $a = 5.0089(5)$, $b = 13.386(1)$, $c = 17.349(2)$ Å, $\alpha = 83.817(8)$, $\beta = 89.80(1)$, $\gamma = 88.04(1)$°, $V = 1155.8(2)$ Å^3, $Z = 3$, $\rho_{calcd} = 1.226$ g cm^{-3}, $\mu = 0.069$ mm^{-1}, 9301 reflections measured, 5192 unique, 418 parameters refined, $\Delta\rho_{max} = 0.29$ e Å^{-3}, $R_1 = 0.061$ (4139 with $[I > 2\sigma(I)]$), $_wR = 0.133$ (all data).

Crystal data for **1b**: Crystal dimensions: $0.40 \times 0.04 \times 0.01$ mm, $C_{26}H_{28}$, $M = 340.51$, $T = 173$ K, triclinic, space group $P\bar{1}$, $a = 3.9992(4)$, $b = 9.4908(1)$, $c = 12.9789(9)$ Å, $\alpha = 69.22(2)$, $\beta = 87.00(2)$, $\gamma = 78.94(2)$°, $V = 451.94(6)$ Å^3, $Z = 1$, $\rho_{calcd} = 1.251$ g cm^{-3}, $\mu = 0.070$ mm^{-1}, 3665 reflections measured, 2014 unique, 174 parameters refined, $\Delta\rho_{max} = 0.39$ e Å^{-3}, $R_1 = 0.056$ (1658 with $[I > 2\sigma(I)]$), $_wR = 0.138$ (all data).

Crystal data for **1c**: Crystal dimensions: $0.40 \times 0.04 \times 0.01$ mm, $C_{30}H_{36}$, $M = 396.61$, $T = 223$ K, triclinic, space group $P\bar{1}$, $a = 5.058(4)$, $b = 9.292(8)$, $c = 12.800(10)$ Å, $\alpha = 103.76(2)$, $\beta = 90.45(4)$, $\gamma = 104.02(2)$°, $V = 565.6(7)$ Å^3, $Z = 1$, $\rho_{calcd} = 1.164$ g cm^{-3}, $\mu = 0.065$ mm^{-1}, 4576 reflections measured, 2014 unique, 208 parameters refined, $\Delta\rho_{max} = 0.22$ e Å^{-3}, $R_1 = 0.076$ (1775 with $[I > 2\sigma(I)]$), $_wR = 0.160$ (all data).

Crystal data for **1d**-form A: Crystal dimensions: $0.50 \times 0.03 \times 0.03$ mm, $C_{34}H_{44}$, $M = 452.72$, $T = 223$ K, monoclinic, space group $C2/c$, $a = 33.27(4)$, $b = 4.739(4)$, $c = 21.54(2)$ Å, $\beta = 90.45(4)$, $\gamma = 127.46(1)$°, $V = 2695(5)$ Å^3, $Z = 4$, $\rho_{calcd} = 1.116$ g cm^{-3}, $\mu = 0.062$ mm^{-1}, 10890 reflections measured, 3056 unique, 242 parameters refined, $\Delta\rho_{max} = 0.35$ e Å^{-3}, $R_1 = 0.086$ (1613 with $[I > 2\sigma(I)]$), $_wR = 0.185$ (all data).

Crystal data for **1d**-form B: Crystal dimensions: $0.50 \times 0.12 \times 0.05$ mm, $C_{34}H_{44}$, $M = 452.72$, $T = 223$ K, triclinic, space group $P\bar{1}$, $a = 5.392(6)$, $b = 8.66(1)$, $c = 15.19(2)$ Å, $\alpha = 101.41(3)$, $\beta = 90.45(4)$, $\gamma = 99.35(6)$°, $V = 673(1)$ Å^3, $Z = 1$, $\rho_{calcd} = 1.116$ g cm^{-3}, $\mu = 0.062$ mm^{-1}, 5358 reflections measured, 2959 unique, 242 parameters refined, $\Delta\rho_{max} = 0.38$ e Å^{-3}, $R_1 = 0.084$ (2045 with $[I > 2\sigma(I)]$), $_wR = 0.209$ (all data).

Crystal data for **1e**: Crystal dimensions: $0.12 \times 0.10 \times 0.05$ mm, $C_{38}H_{52}$, $M = 508.83$, $T = 223$ K, triclinic, space group $P\bar{1}$, $a = 5.146(4)$, $b = 11.28(1)$, $c = 13.55(1)$ Å, $\alpha = 85.63(2)$, $\beta = 84.72(3)$, $\gamma = 81.70(3)$°, $V = 773(1)$ Å^3, $Z = 1$, $\rho_{calcd} = 1.092$ g cm^{-3}, $\mu = 0.061$ mm^{-1}, 6174 reflections measured, 3466 unique, 276 parameters refined, $\Delta\rho_{max} = 0.25$ e Å^{-3}, $R_1 = 0.065$ (2048 with $[I > 2\sigma(I)]$), $_wR = 0.164$ (all data).

Crystal data for **1f**: Crystal dimensions: $0.33 \times 0.05 \times 0.01$ mm, $C_{42}H_{60}$, $M = 564.90$, $T = 173$ K, monoclinic, space group $C2/c$, $a = 33.04(3)$, $b = 4.735(3)$, $c = 26.41(2)$ Å, $\beta = 123.586(8)$°, $V = 3442(5)$ Å^3, $Z = 4$, $\rho_{calcd} = 1.090$ g cm^{-3}, $\mu = 0.060$ mm^{-1}, 13423 reflections measured, 3891 unique, 190 parameters refined, $\Delta\rho_{max} = 0.22$ e Å^{-3}, $R_1 = 0.136$ (2245 with $[I > 2\sigma(I)]$), $_wR = 0.232$ (all data).

Calculations: The lowest-energy absorption band of the tetracene molecule, on the basis of geometry obtained by X-ray analysis, was calculated using the TD-DFT B3LYP/6-31G* method with Gaussian 03.[16] The exciton displacement energy ($\Delta E_{exciton}$), corresponding to the spectral shift between a pair of molecules, is given by the following dipole-dipole equation: $\Delta E_{exciton} = |\mu|^2(1-3\cos^2\theta)/r^3$, where μ is the transition dipole and θ and r are the angle and distance between two transition dipoles, respectively.[17] The term $|\mu|^2$ directly depends on the absorption coefficient of the molecule. The term $(1-3\cos^2\theta)/r^3$ determines the geometrical relationship of transition dipoles correlated with the crystal structure. Whether a shift is blue or red depends on the critical angle $\theta = 54.7$°, above which the shift is blue and below which the shift is red. μ was calculated by the TD-DFT calculations, and the θ and r were obtained from the geometry of the crystal structures. Calculations of $\Delta E_{exciton}$ were performed on the nearest-neighbor molecules within 20 Å. The total energy displacement was then summed up to be E_{shift}.

Acknowledgements

The authors are grateful to Prof. Dr. Shinya Matsumomo (Yokohama National University) for discussions about intermolecular interactions. We also thank the Instrument Center of the Institute for Molecular Science for X-ray structural analyses. This work was supported by a Grant-in-Aid (No. 20550128) from the Ministry of Education, Culture, Sports, Science and Technology, Japan.

[1] a) M. Bendikov, F. Wudl, D. F. Perepichka, *Chem. Rev.* **2004**, *104*, 4891; b) J. E. Anthony, *Angew. Chem.* **2008**, *120*, 460; *Angew. Chem. Int. Ed.* **2008**, *47*, 452.

[2] a) A. S. Paraskar, A. R. Reddy, A. Patra, Y. H. Wijsboom, O. Gidron, L. J. W. Shimon, G. Leitus, M. Bendikov, *Chem. Eur. J.* **2008**, *14*, 10639; b) Z. Chen, P. Müller, T. M. Swager, *Org. Lett.* **2006**, *8*, 273; c) R. Schmidt, S. Göttling, D. Leusser, D. Stalke, A.-M. Krause, F. Würthner, *J. Mater. Chem.* **2006**, *16*, 3708; d) J. Reichwagen, H. Hopf, A. Del Guerzo, J.-P. Desvergne, H. Bouas-Laurent, *Org. Lett.* **2005**, *7*, 971; e) J. A. Merio, C. R. Newman, C. P. Gerlach, T. W. Kelley, D. V. Muyres, S. E. Fritz, M. F. Toney, C. D. Frisbie, *J. Am. Chem. Soc.* **2005**, *127*, 3997; f) S. A. Odom, S. R. Parkin, J. E. Anthony, *Org. Lett.* **2003**, *5*, 4245.

[3] a) I. Kaur, W. Jia, R. P. Kopreski, S. Selvarasah, M. R. Dkmeci, C. Pramanik, N. E. McGruer, G. P. Miller, *J. Am. Chem. Soc.* **2008**, *130*, 16274; b) D. Lehnherr, R. McDonald, R. R. Tykwinski, *Org. Lett.* **2008**, *10*, 4163; c) Y.-M. Wang, N.-Y. Fu, S.-H. Chan, H.-K. Lee, H. N. C. Wong, *Tetrahedron* **2007**, *63*, 8586; d) J. E. Anthony, J. Giershner, C. A. Landis, S. R. Parkin, J. B. Sherman, R. C. Bakus II, *Chem. Commun.* **2007**, 4746; e) Q. Miao, X. Chi, S. Xiao, R. Zeis, M. L. Lefenfeld, T. Siegrist, M. L. Steigerwald, C. Nuckolls, *J. Am.*

Chem. Soc. **2006**, *128*, 1340; f) T. Takahashi, S. Li, W. Huang, F. Kong, K. Nakajima, B. Shen, T. Ohe, K. Kanno, *J. Org. Chem.* **2006**, *71*, 7967; g) K. Kobayashi, R. Shimaoka, M. Kawahata, M. Yamanaka, K. Yamaguchi, *Org. Lett.* **2006**, *8*, 2385; h) J. Jiang, B. R. Kaafarani, D. C. Neckers, *J. Org. Chem.* **2006**, *71*, 2155; i) M. A. Wolak, B.-B. Jang, L. C. Palilis, Z. H. Kafafi, *J. Phys. Chem. B* **2004**, *108*, 5492.

[4] C. Kitamura, Y. Abe, N. Kawatsuki, A. Yoneda, K. Asada, T. Kobayashi, H. Naito, *Mol. Cryst. Liq. Cryst.* **2007**, *474*, 119.

[5] a) G. Klebe, F. Graser, E. Hädicke, J. Berndt, *Acta Crystallogr. Sect. B* **1989**, *45*, 69; b) F. Graser, E. Hädicke, *Liebigs Ann. Chem.* **1984**, 483; c) F. Graser, E. Hädicke, *Liebigs Ann. Chem.* **1980**, 1994.

[6] C. Kitamura, T. Ohara, N. Kawatsuki, A. Yoneda, T. Kobayashi, H. Naito, T. Komatsu, T. Kitamura, *CrystEngComm* **2007**, *9*, 644.

[7] G. W. Gribble, R. B. Perni, K. D. Onan, *J. Org. Chem.* **1985**, *50*, 2934.

[8] Y. Himeshima, T. Sonoda, H. Kobayashi, *Chem. Lett.* **1983**, 1211.

[9] H. Pellissier, M. Santelli, *Tetrahedron* **2003**, *59*, 701.

[10] See, for example: a) Z. Liu, R. C. Larock, *J. Org. Chem.* **2007**, *72*, 223; b) S. Bhuvaneswari, M. Jeganmohan, C.-H. Cheng, *Org. Lett.* **2006**, *8*, 5581; c) C. Romero, D. Pēna, D. Pérez, E. Guitián, *Chem. Eur. J.* **2006**, *12*, 5677; d) J. Ikadai, H. Yoshida, J. Ohshima, A. Kunai, *Chem. Lett.* **2005**, *34*, 56.

[11] H. M. Duong, M. Bendikov, D. Steiger, Q. Zhang, G. Sonmez, J. Yamada, F. Wudl, *Org. Lett.* **2003**, *5*, 4433.

[12] R. G. Cooke, B. L. Johnson, W. R. Owen, *Aust. J. Chem.* **1960**, *13*, 256.

[13] See, for example: a) Y. Kikkawa, E. Koyama, S, Tsuzuki, K. Fujiwara, K. Miyake, H. Tokuhisa, M. Kanesato, *Chem. Commun.* **2007**, 1343; b) N. Fujita, Y. Sakamoto, M. Shirakawa, M. Ojima, A. Fujii, M. Ozaki, S. Shinkai, *J. Am. Chem. Soc.* **2007**, *129*, 4134.

[14] J. Bernstein, *Polymorphism in Molecular Crystals*, Clarendon Press, Oxford, **2002**.

[15] P. M. Kazmaier, R. Hoffmann, *J. Am. Chem. Soc.* **1994**, *116*, 9684.

[16] Gaussian 03, Revision C.02, M. J. Frisch, G. W. Trucks, H. B. Schlegel, G. E. Scuseria, M. A. Robb, J. R. Cheeseman, J. A. Montgomery, Jr., T. Vreven, K. N. Kudin, J. C. Burant, J. M. Millam, S. S. Iyengar, J. Tomasi, V. Barone, B. Mennucci, M. Cossi, G. Scalmani, N. Rega, G. A. Petersson, H. Nakatsuji, M. Hada, M. Ehara, K. Toyota, R. Fukuda, J. Hasegawa, M. Ishida, T. Nakajima, Y. Honda, O. Kitao, H. Nakai, M. Klene, X. Li, J. E. Knox, H. P. Hratchian, J. B. Cross, C. Adamo, J. Jaramillo, R. Gomperts, R. E. Stratmann, O. Yazyev, A. J. Austin, R. Cammi, C. Pomelli, J. W. Ochterski, P. Y. Ayala, K. Morokuma, G. A. Voth, P. Salvador, J. J. Dannenberg, V. G. Zakrzewski, S. Dapprich, A. D. Daniels, M. C. Strain, O. Farkas, D. K. Malick, A. D. Rabuck, K. Raghavachari, J. B. Foresman, J. V. Ortiz, Q. Cui, A. G. Baboul, S. Clifford, J. Cioslowski, B. B. Stefanov, G. Liu, A. Liashenko, P. Piskorz, I. Komaromi, R. L. Martin, D. J. Fox, T. Keith, M. A. Al-Laham, C. Y. Peng, A. Nanayakkara, M. Challacombe, P. M. W. Gill, B. Johnson, W. Chen, M. W. Wong, C. Gonzalez, J. A. Pople, Gaussian, Inc., Wallingford CT, **2004**.

[17] a) M. Kasha, *Spectroscopy of the Excited State*, Plenum Press, New York, **1976**; b) M. Kasha, H. R. Rawls, M. Ashraf El-Bayoumi, *Pure Appl. Chem.* **1965**, *11*, 371.

[18] J. M. Ribó, J. M. Bofill, J. Crusats, R. Rubires, *Chem. Eur. J.* **2001**, *7*, 2733.

[19] S. Matsumoto, W. Tokunaga, H. Miura, J. Mizuguchi, *Bull. Chem. Soc. Jpn.* **2001**, *74*, 471.

[20] J. Mizuguchi, *J. Phys. Chem. A* **2000**, *104*, 1817.

[21] J. V. Morris, M. A. Mahaney, J. R. Huber, *J. Phys. Chem.* **1976**, *80*, 969.

[22] A. Altomare, M. C. Burla, M. Camalli, M. Cascarano, C. Giacovazzo, A. Guagriardi, G. Polidor, *J. Appl. Crystallogr.* **1994**, *27*, 435.

[23] G. M. Sheldrick, *Acta Crystallogr. Sect. A* **2008**, *64*, 112.

[24] teXsan, Crystal Structure Analysis Package, Molecular Structure Corporation **1985** and **1999**.

Received: June 18, 2009
Published online: November 20, 2009

